Dispersion Strengthened Superalloys by Mechanical Alloying

JOHN S. BENJAMIN

A new process called "mechanical alloying" has been developed which produces homogeneous composite particles with an intimately dispersed, uniform internal structure. Materials formed by hot consolidation of this powder achieve the long-sought combination of dispersion strengthening and age-hardening in a high temperature alloy. While the process is amenable to making a variety of alloys, its first use has been to combine yttrium oxide and gamma prime hardening in a complex nickel-base superalloy. Typical stress rupture properties are 40,000 psi for 100 hr at 1400°F and 15,000 psi for 100 hr at 1900°F together with excellent sulfidation and cyclic oxidation resistance. From a fundamental standpoint, results show that the age-hardening dominates the low-temperature strength, dispersion strengthening dominates at high temperature, and the two are augmentative in the intermediate temperature range 1300° to 1500°F.

THE use of inert additions to improve elevated temperature mechanical properties in metals was first exploited in 1910 by W. D. Coolidge[1] in thoriated tungsten. The fact that other minor additions or "dopants" could also increase creep resistance was soon discovered. These materials were mainly designed for sag resistance, requiring the strength to support their own weight for very long times at high temperatures.

The first dispersion strengthened material designed as a structural load bearing system was SAP.[2] A dispersion of aluminum oxide flakes in aluminum conferred strength in this system up to the melting point of the aluminum matrix. Studies showed[3,4] that the strength of this material increased with increasing volume fraction of the oxide and with decreasing interparticle spacing. The relatively low melting point of aluminum, however, represents a severe limitation for use at elevated temperatures. This led to attempts to apply dispersion strengthening to higher melting point bases such as copper and nickel.[5] In these metals, the self oxides cannot be used as they are not sufficiently stable against Ostwald ripening growth at elevated temperatures. Even though the problems of establishing a fine dispersion of sufficiently refractory oxide in a high melting metal matrix, for example ThO_2 in nickel, were solved,[6] and mechanical working techniques giving vastly improved high temperature strength were developed,[7] the resulting dispersion strengthened metals were still limited in their usefulness by their low strength at intermediate temperature and lack of corrosion resistance.

While some success has been achieved in producing a dispersion strengthened corrosion resistant alloy with an 80 Ni-20 Cr matrix this alloy still suffers from relatively low intermediate temperature creep strength.

Hypothetically these shortcomings could be solved by combining the corrosion resistance and intermediate temperature strength of γ' precipitation hardened nickel-base superalloys with the high temperature strength and stability of oxide dispersion strengthening. The primary hurdle to be overcome to make such a material is the production of a dispersion of fine refractory oxide particles less than 0.1 μ in size upon or within an alloy powder particle in such a manner as to lead to interparticle spacings of less than 0.5 μ in a consolidated product.

It is a well known fact that the most effective precipitation hardening elements in nickel-base alloys, aluminum, titanium, and niobium, are easily oxidized. Their oxidation would remove them as precipitation hardeners. Therefore, oxygen contamination must be kept low enough to leave sufficient γ' formers in a reduced state to give adequate age hardening for intermediate temperature strength. In addition the combination of effective oxide dispersion strengthening and precipitation hardening must be accomplished at a reasonable cost.

There are four major techniques which have been used previously to combine oxide dispersion strengthening and solid solution strengthening in alloy systems containing relatively nonreactive elements. A brief consideration of the nature and limitations of each of these techniques will show why they are not suited to the task of producing an alloy containing γ':

Simple mechanical mixing involves the use of a high speed blender[8,9] or a ball mill[10] to coat the surface of a metal or alloy powder with oxide powders. The interparticle spacing in the consolidated alloy produced from these powders is limited by the starting metal powder particle size. Powder sizes of less than 5 μ are required to get sufficiently fine interparticle spacings even with large mechanical reductions during consolidated and subsequent working operations. Powders this fine containing γ' formers such as aluminum and titanium are very reactive because of their high specific surface area and complete or nearly complete oxidation of aluminum and titanium can result.

Ignition surface coating technique[11] involves mixing matrix alloy powders with a liquid solution of a salt of a reactive metal. This mixture is dried and pulverized and the powders are heated in an inert or reducing environment converting the salt to a refractory oxide. This technique also produces oxide coated powders which have, therefore, the same disadvantages as powders produced by the simple mechanical mixing technique. In addition, there is a greater contamination problem because of the oxidizing potential of the reaction products of the salt decomposition step.

Internal oxidation technique[12-17] involves exposing

JOHN S. BENJAMIN is Supervisor, Composites Section, Paul D. Merica Research Laboratory, The International Nickel Co., Sterling Forest, Suffern, N. Y.

Manuscript submitted February 2, 1970.

metal powders or thin metal strip containing a dilute solid solution of a reactive element to an oxidizing environment at elevated temperatures. The reactive element is converted to a dispersoid by diffusing oxygen.

It has been found experimentally[17] that the particle size of the dispersoid increases with increasing depth of penetration of the internal oxidation front into the metal. Very fine, contamination-prone powders or expensive ultra-thin strip are required to obtain sufficiently fine dispersoid particle sizes. In the case where the alloy also contains reactive γ' forming elements such as titanium and aluminum, an additional problem would arise. The oxygen potential could not be raised above the extremely low values required to oxidize the γ' forming elements and the oxidation rate of the desired dispersoid forming elements would be prohibitively slow.

Selective reduction process[6] has been used to manufacture commercial dispersion strengthened materials. It involves producing an intimate mixture of metal oxides, and selectively reducing the oxides of the matrix alloy while leaving the dispersoid unreduced. If aluminum and titanium are to be present in the matrix alloy, the reduction step is not possible with gases because of the stability of Al_2O_3 and TiO_2. These oxides can be reduced by the use of molten alkali and alkaline earth metals. However, this introduces two major new problems: excessive growth of the dispersoid particles, and the necessity to remove the reaction product oxides and carrier agent, usually a salt.

In this present investigation a new "mechanical alloying" technique has been developed which circumvents the previous shortcomings and permits the effective combination of oxide dispersion strengthening and γ' precipitation hardening in nickel-base superalloys.

EXPERIMENTAL PROCEDURE

Raw Materials

The raw materials used in this study were Type 123 carbonyl nickel powder of 4 to 7 μ particle size, chromium powder of –200 mesh size, dispersoids consisting of thorium oxide and yttrium oxide of 100 to 500Å particle sizes, and Ni-Al-Ti vacuum-melted master alloy crushed to powders of –200 mesh particle size. The master alloy powders were employed to reduce the reactivity of aluminum and titanium below that of their elemental powder forms. This technique is commonly used in pyrometallurgy for the addition of volatile elements. The thermodynamic activities (partial pressures) of the reactive elements are reduced by first alloying them with one of the major constituents of the alloy. An example is the addition of nickel-zirconium to a molten nickel-base alloy. The master alloy technique has also been previously employed in powder metallurgy in the production of alloys containing a reactive component.[18]

In the Ni-Al system, it has been shown that the activity coefficient of aluminum is 1.8×10^{-4} on the nickel-rich side of the intermetallic compound NiAl at 1800°F.[19] The activity of aluminum in this compound is reduced nearly ten-thousand fold beyond a simple Raoult's law dilution. This effect was used to protect the aluminum and titanium additions to the alloys in this study by using a compound consisting of 65 at. pct Ni and 35 at. pct of the sum of Al and Ti. Zirconium and boron were also added as master alloys.

Equipment and Processing

The alloy powders produced in this study were processed in Model 1-S and 10-S Szegvari Attritor Grinding Mills*[20,21] designed for paint and ink production. These machines are high energy driven ball mills in which the charge of balls and powder is held in a stationary, vertical, water cooled tank and agitated by impellers radiating from a rotating central shaft.

* Registered Trademark of Union Process, Inc.

The attritor charge consisted of 10 kg of powder with 175 kg of +0.6 cm nickel pellets. Unless otherwise specified, batches were processed at 132 rpm for 40 hr in a sealed air atmosphere. After screening to remove the coarse +45 mesh particles, the remaining powder was packed in steel extrusion cans, evacuated to less than 0.01 μ at 750°F and sealed by fusion welding. The powders were consolidated by hot extrusion in a conventional 750 ton extrusion press at temperatures of 2150°F or below with extrusion ratios of 12:1 or greater.

Unless otherwise stated specimens were heat treated as follows: 2 hr at 2325°F in argon, air cool; 7 hr at 1975°F in air, air cool; 16 hr at 1300°F in air, air cool. The first treatment was for homogenization and grain growth while the last two treatments were conventional nickel-base superalloy solution and aging treatments.

Standard techniques were employed in metallographic specimen preparation. Elevated temperature tensile and stress rupture tests were performed in air according to ASTM specifications E21-66T and E139-66T.

EXPERIMENTAL RESULTS AND DISCUSSION

Results and their discussion fall into two interrelated categories: evaluation of the mechanical alloying process, and characteristics of the resulting dispersion strengthened, precipitation hardened superalloys.

Mechanical Alloying Process

The dispersion strengthened alloys for this study were made by the dry, high energy mechanical alloying technique. The key features of this process are the high energy milling and the *omission* of any surface active agent other than the air sealed into the attritor tank with the charge. This practice actually promotes particle welding in contrast to conventional metal ball milling practices in which welding is inhibited by use of liquids and surfactants.

The nature of the mechanical alloying process can best be understood by reference to the internal structures of powder particles processed for varying lengths of time with all other processing conditions held fixed. In order to illustrate the rate of development of the composite particle structure, batches of powder were processed for six time intervals from 1.5 to 40 hr duration. Photomicrographs originally taken at 250X of samples of powder from these batches are shown in Fig. 1. Fig. 1(*a*) shows the structure of powder processed for 1.5 hr. Note that the formation of composite metal particles has begun. Many of these particles are

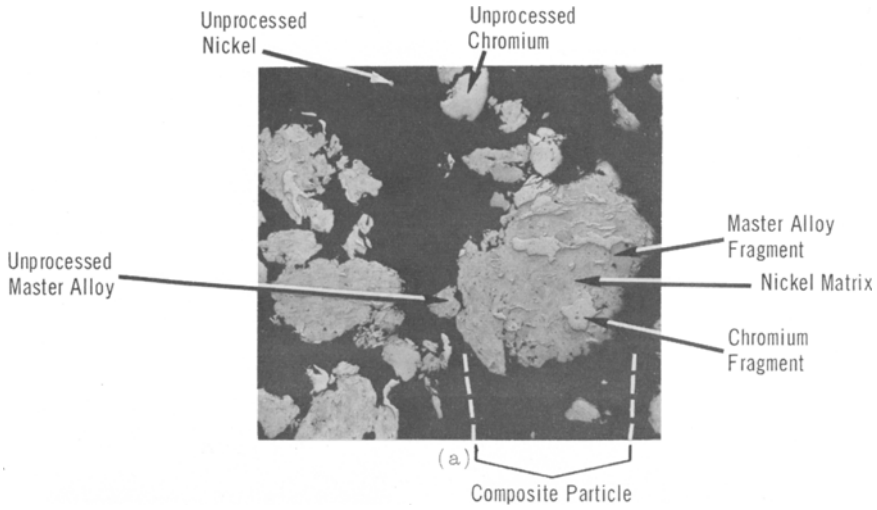

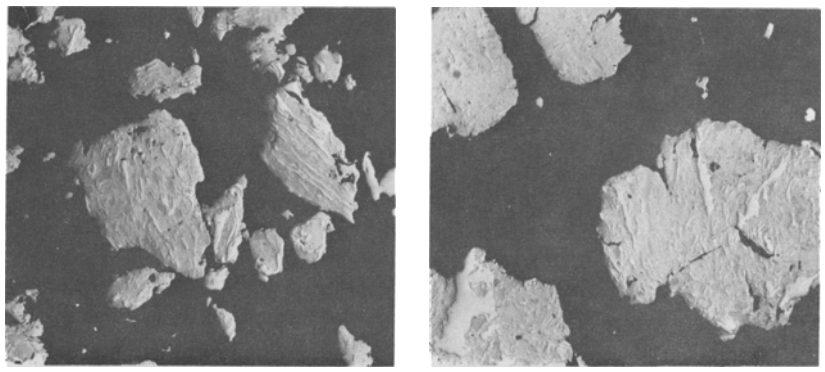
(b)

(c)

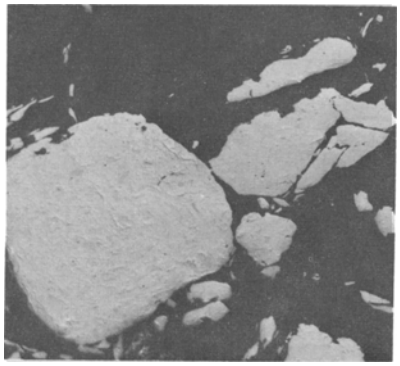
(d)

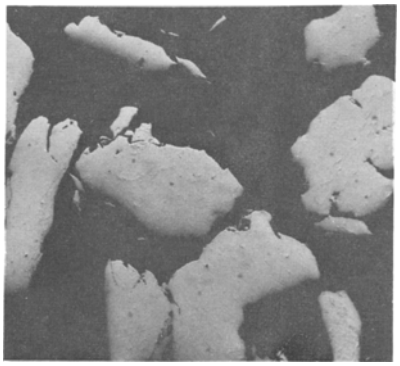
(e)

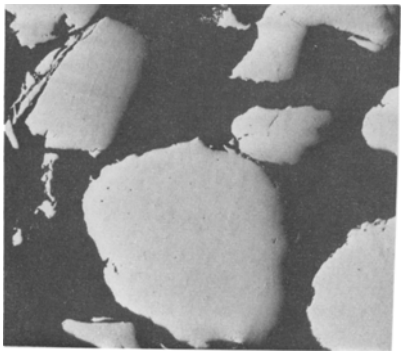
(f)

Fig. 1—Structures of composite powders processed for various times in a 10-S attritor operated at 132 rpm. Ball charge: 175 kg of +.6 cm nickel pellets; 10 kg of powders. (*a*) 1.5 hr; (*b*)3.5 hr; (*c*)9.5 hr; (*d*) 20 hr; (*e*)30 hr; (*f*) 40 hr. Magnification 163 times.

larger than the coarsest starting materials which were 74 μ in size. Unprocessed particles of the major constituents and the presence of processed fragments within the composite particles can be identified. Examples of these features are labeled in Fig. 1(*a*). Unprocessed nickel is identified by its small size and relatively equiaxed cross section. The larger, single-phase, light particles are unprocessed chromium. The master alloy powders can be identified by the fact that they are two-phased. Within the composite particles the chromium fragments stand in strong relief against the light gray nickel matrix. The darker phase of the master alloy can also be seen.

The dispersoid which was added in the amount of 2.5 vol pct cannot be detected in these photomicrographs. This oxide was formed by the thermal decomposition of a less stable compound of the reactive metal. The decomposition product consisted of very fine 100 to 500Å oxide crystallites arranged in tightly agglomerated pseudomorphs having the approximate size and shape of the compound particles prior to calcination. These agglomerates, originally up to 20 μ in size, have been

sufficiently broken apart by the mechanical alloying process that the resulting ultrafine oxide crystallites, distributed along weld interfaces within the material, cannot be resolved by the optical microscope.

With increasing processing time the structure of the composite particles becomes more uniform, its striated nature, as delineated by the chromium platelets becomes more apparent and unprocessed powders are less plentiful. The shape of the chromium fragments then becomes more equiaxed than at shorter times and both the spacing and the size of the fragments are much smaller.

After 20 hr of processing, see Fig. 1(*d*), no large chromium fragments are present within the composite particles. The structures of both large and small composite particles are similar. With further processing an increasing proportion of the chromium fragments within these particles become reduced in size below the resolving power of the optical microscope, about 0.5 μ. Powders processed for 40 hr, see Fig. 1(*f*), and longer are, therefore, relatively featureless. It is likely, however, that refinement of the structure continues with increasing processing time but on a level below that of optical resolution.

The mechanical alloying process involves the welding of the various powder constituents to the grinding charge pellets. An irregular welded layer is built up which constantly flaked off the balls, fragmented and rewelded. At each of these weld-flaking cycles of the process the dimensions of the constituent fragments are reduced 5 to 10 fold in their smallest dimension. Fig. 2 shows a section through a ball withdrawn at an intermediate stage in the process. Note the welded composite layer and the nickel ball beneath.

When the processing of a batch is complete, a valve on the bottom of the attritor is opened and the machine is run until the entire batch has been dewelded and drained.

The rapid homogenization of structure obtained in the high energy attritor can be contrasted with the rate of processing in a conventional ball mill. The structures developed in the conventional, low energy, 15.25 cm diam ball mill operating dry at 80 rpm under standard conditions of a 3-to-1 ball-to-powder ratio and with a higher 6-to-1 ball-to-powder ratio for 32 and 125 hr are shown in Fig. 3.

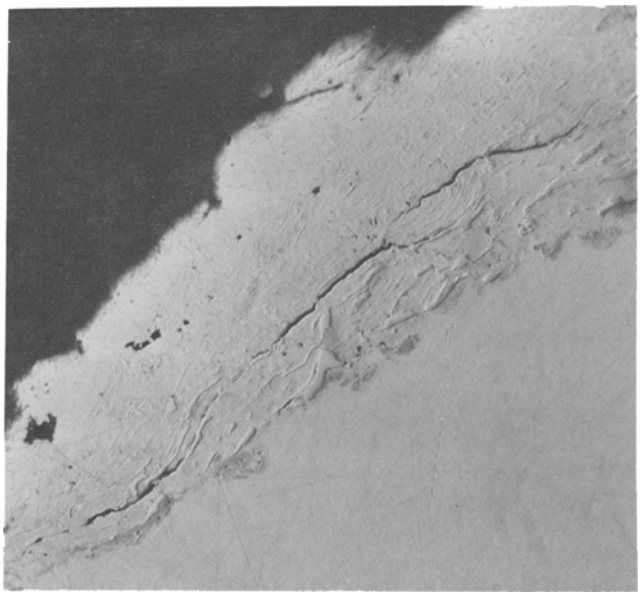

Fig. 2—Surface of sectioned nickel pellet showing welded composite layer. Magnification 260 times.

The structure of powders of the yttriated superalloy composition processed for 32 hr with a 3-to-1 ball-to-powder ratio are shown in Fig 3(*a*). Most of the material is unchanged from its starting size. Within the few agglomerates which occur even the original nickel particles can be identified by outlines of refractory oxide pseudomorph fragments near the revolving power of the optical microscope in size, see circled area in Fig.

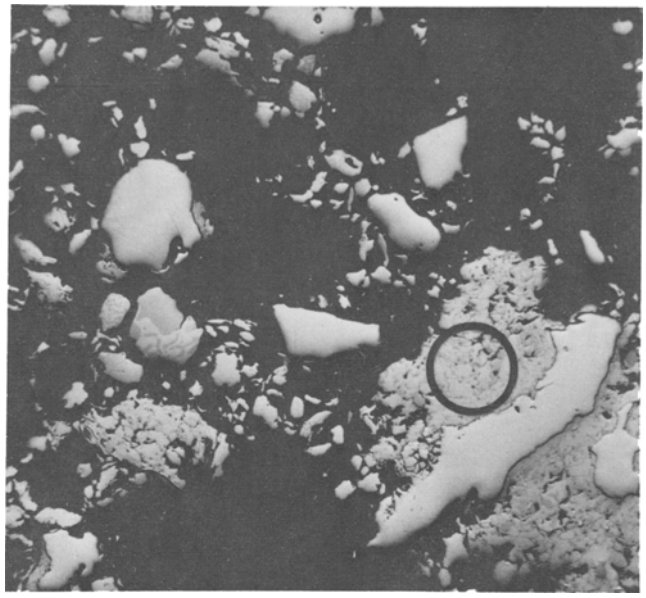

(*a*)

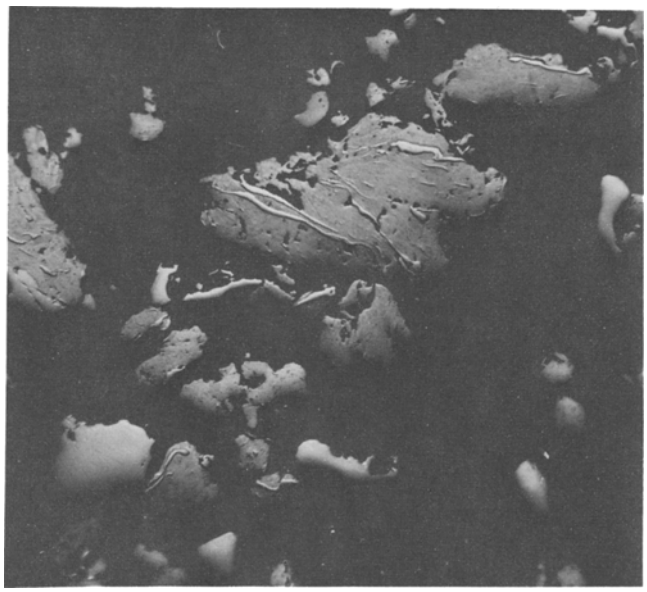

(*b*)

Fig. 3—Structures of composite powders processed for various times in conventional ball mill operated at 80 rpm. Area of nickel particles outlined by oxide pseudomorph fragments is circled in (*a*). (*a*) 32 hr, 3-to-1 ball-to-powder ratio; (*b*) 125 hr, 3-to-1 ball-to-powder ratio; (*c*) 32 hr, 6-to-1 ball-to-powder ratio; (*d*) 125 hr, 6-to-1 ball-to-powder ratio. Magnification 240 times.

(c)

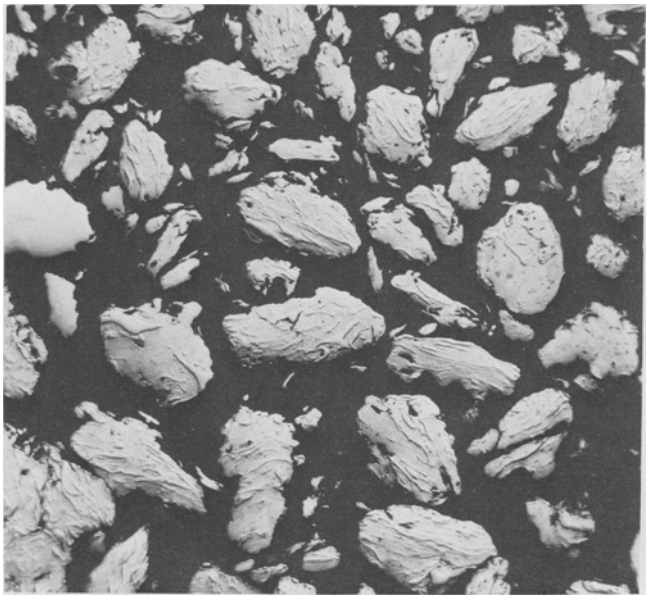

(d)

Fig. 3—Continued

3(*a*). These nickel particles are relatively equiaxed in shape. The ball milled agglomerates are easily broken apart by a Vickers' microhardness indentor with a 100 g load while composite particles processed 40 hr in the attritor withstood at least a 500 g load. These observations suggest that the agglomerates from the conventional ball mill are held together by weak mechanical interlocking rather than by cold welding typical of high energy milling.

Powder processed for 125 hr in a 15.25 cm ball mill with a 3-to-1 ball-to-powder ratio, see Fig. 3(*b*), does show evidence of welding and has an appearance similar to powder processed for 1.5 hr in the attritor, see Fig. 1(*a*).

Batches of yttriated superalloy powder were also processed in a 15.25 cm ball mill with a higher 6-to-1, ball-to-powder ratio. The structure of powders processed for 32 hr is shown in Fig. 3(*c*). While a few welded composite particles are present, the majority of the powder is unprocessed and the structure is less homogeneous than that of powder processed for 1.5 hr in the attritor. After 125 hr of processing in a ball mill with a 6-to-1 ball-to-powder ratio, see Fig. 3(*d*), the structure is approximately equivalent to that of powders processed for 3.5 hr in the attritor, see Fig. 1(*b*). It is clear that an extremely long time would be required to obtain the desired homogeneity with conventional ball milling if, in fact, such milling would ever result in suitable powders.

These differences in processing rates in an attritor and a conventional ball mill are directly related to the relative efficiency of the mills and the energy input rate achieved in the two mills. The maximum operating speed of a conventional ball mill is a function of the diameter of the mill. Centrifugal pinning of balls and powders occurs at higher rotation speeds.[22] The attritor, in which the energy is imparted to the balls by the passage of rotating impellers through the ball charge and not by rotating the entire machine, can be run at especially high speeds. For example, the critical speed for a 40.6 cm diam ball mill is about 63 rpm and such a mill would normally be run at 43 rpm. A 40.6 cm diam attritor is typically operated at speeds between 125 and 185 rpm.

In the foregoing, the mechanical alloying process has been related to the phenomenon of cold welding, a process long used to join metals on the macroscopic scale.[23] It is known that a true metallurgical bond is formed when two pieces of metal sheet which have been cleaned of grease and gross oxides are placed together and compressively deformed to true strains in excess of 1.0. This is demonstrated by the fact that failure of the welded pieces occurs by tearing of the parent metal rather than separation at the weld interface. It is also known that a mild coating or welding action can occur in conventional ball milling and this fact is employed in the production of tungsten carbide-cobalt materials.[24] However, the degree to which the phenomen occurs in tungsten-carbide-cobalt production is slight and the processing times required are very long.

The relative ease of welding an alloy in ball milling can be estimated by the ease of cold welding sheet of the same material. This in turn is a function of the ratio of the milling temperature to the melting point of the material. It can be shown that low melting metals such as lead and aluminum can be cold welded very easily at room temperature and that they also demonstrate a great tendency to weld during conventional milling. However, higher melting point metals such as copper, iron, and nickel are much more difficult to cold weld in macroscopic form, requiring 5 to 20 times as much energy input per weld as aluminum and lead. Similarly, they cannot be welded at reasonable rates in a conventional ball mill, but can be readily welded in a high energy mill.

A uniform fine dispersion of refractory oxide particles can be established by the mechanical alloying process *within* relatively coarse composite powder particles containing reactive elements such as aluminum and titanium while limiting oxygen contamination to acceptable levels. Coarse elemental and partially prealloyed powders, which are stable and relatively inexpensive, can be employed to produce mechanically alloyed particles, chemically homogeneous on a submicron scale. The spacings of compositional variations

Table I. Compositions of Experimental Dispersion Strengthened Nickel-Base Superalloys

Alloy	C	Al	Ti	Cr	Mo	Nb	Zr	B	ThO_2	Y_2O_3	Al_2O_3
A	0.061	0.92	2.46	20.4	–	–	0.029	0.005	–	1.22	0.37
B	0.049	0.96	2.77	18.7	–	–	0.09	0.003	–	1.33	0.99
C	0.056	0.90	2.33	20.6	–	–	0.065	0.005	–	1.22	0.83
D	0.055	0.74	2.10	19.0	–	–	0.025	0.002	2.71	–	1.30
E	0.069	4.19	0.82	10.4	3.0	1.6	0.03	0.007	3.00	–	1.38

are actually less than those found in many castings. The dispersion of all the oxides present including any possible contaminants, is very fine and is achieved in a relatively short time.

Dispersion Strengthened Superalloys

Nothing in the preceding consideration of the mechanical alloying mechanism suggests that it is restricted to any particular alloy base. While a wide variety of products can be made with this process, we shall concentrate here on thoriated and yttriated nickel-base superalloys. The compositions of some of the superalloys which have been produced by the mechanical alloying process are given in Table I.

Structure

Typical longitudinal and transverse microstructures of the yttriated superalloy, Alloy A, Table I, after extrusion and heat treatment are shown in Fig. 4. The heat treatment consisted of a grain coarsening anneal, 2 hr at 2325°F; solution treatment, 7 hr at 1975°F; and aging, 16 hr at 1300°F. The grain structure of the dispersion strengthened superalloys in the partially and fully heat treated conditions consists of elongated cylindrical grains of very irregular cross section. The long axes of the grains are parallel to the extrusion axis of the bar. Such elongated structures have previously been shown to give superior elevated temperature properties in dispersion strengthened materials.[25] This has also been found to be true of the dispersion strengthened superalloys considered in this investigation.

Very little else of the structure of the heat treated alloy is revealed by optical microscopy. The γ' and Y_2O_3 are too fine to be resolved and only the carbides or occasional coarse contaminant oxides are visible.

Electron micrographs reveal the copresence of oxide and γ' clearly. Fig. 5 shows the structure at 4950X of a longitudinal section of dispersion strengthened superalloy E, heat treated by annealing 4 hr at 2250°F followed by a furnace cool. Examples of the microstructural features are labeled. Note the grain boundary A-A′ running diagonally across the photograph. There appears to be both carbide and γ' precipitated at this boundary. Because of the higher aluminum content of this alloy, see Table I, and the furnace cooling treatment, the γ' is present as coarse irregular particles as well as a fine secondary precipitate. The remaining dispersion composed of ThO_2, Al_2O_3, and carbide particles is most easily distinguished within the coarse γ' particles. The larger of these dispersoid particles are probably MC carbides and have sizes up to 3000Å. The finer particles with sizes down to at least 100Å, the limit of resolution of the replication technique, are predominantly ThO_2 and Al_2O_3. The majority of these particles are finer than 1000Å and are well within the range required for dispersion strengthening.

Properties

The stress rupture properties of typical yttriated superalloys A and B at temperatures of 1200°, 1400°, 1500°, 1700°, and 1900°F are shown in Fig. 6. The stress rupture properties of thoriated superalloy D at temperatures of 1200°, 1500°, 1700°, 1850°, and 2000°F are shown in Fig. 7. It is interesting to note that the slopes of the stress rupture plots at higher temperatures, 1900° and 2000°F, are less than at lower temperatures, 1200° and 1400°F. This is in direct contrast to the case for conventional nickel-base superalloys

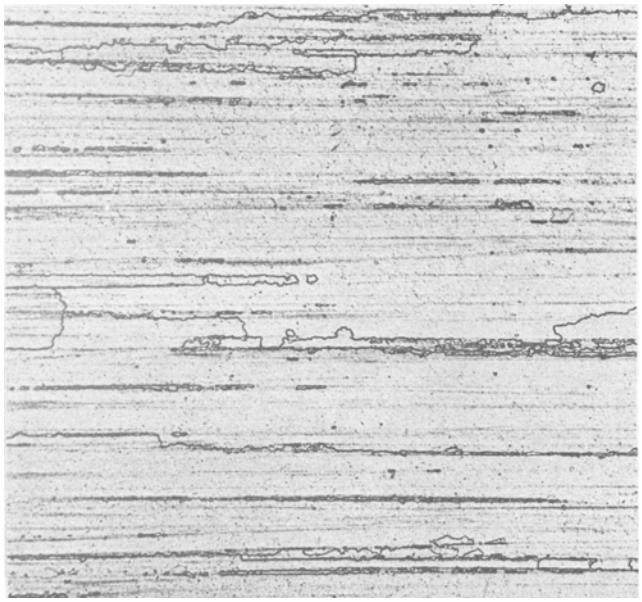

(a)

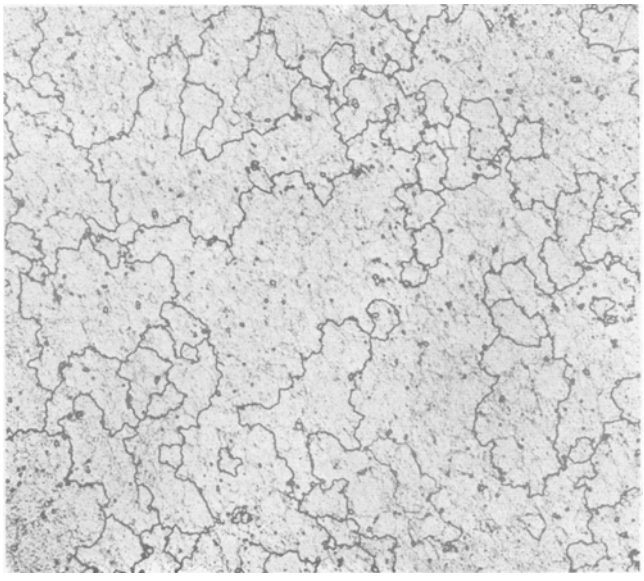

(b)

Fig. 4—Extruded yttriated superalloy (alloy A, Table I). Heat treated: 2325°F/2 hr/AC, 1975°F/7 hr/AC, 1300°F/16 hr/AC. (a) Longitudinal section; (b) transverse section. Magnification 104 times.

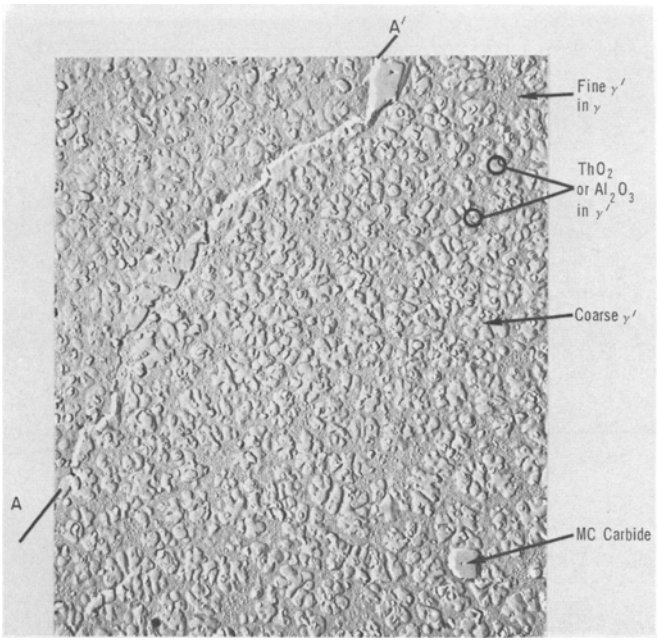

Fig. 5—Electron photomicrograph of surface replica of complex thoriated superalloy (alloy E, Table I). Extruded and heat treated 4 hr at 2250°F followed by a furnace cool. Magnification 4950 times.

where the slopes of the stress rupture plots increase with increasing temperature. This unusual behavior immediately suggests that more than one strengthening mechanism is operating. The elongations at rupture for both yttriated and thoriated superalloys ranged from 1 to 10 pct, the majority of the values being between 2.5 and 7.5 pct.

In order to compare the properties of these alloys with conventionally produced materials, the 100-hr rupture stresses of yttriated and thoriated superalloys are plotted as a function of temperature in Figs. 8 and 9. The 1000-hr rupture stresses of yttriated superalloys are plotted as a function of temperature in Fig. 10. Also included[26] are typical values for TD Nickel,* a commercial dispersion strengthened material, and NIMONIC *80A, a commercial nickel-base superalloy with a composition similar to the matrix composition of the experimental dispersion strengthened superalloys.

*Registered Trademark of Fansteel, Metals Division.

*Registered Trademark of The International Nickel Co., Inc.

The presence of the two strengthening regimes in dispersion strengthened nickel-base superalloys is strikingly demonstrated in Figs. 8 and 9. At temperatures below 1500°F both the yttriated and thoriated superalloys are stronger than thoriated nickel and follow the curve for γ' strengthened NIMONIC 80A very closely. At temperatures above 1500°F the 100-hr rupture stress curves of the yttriated and thoriated superalloys are parallel to that of thoriated (TD) nickel. The apparent superiority of the yttriated superalloy over the thoriated superalloy at temperatures above 1500°F is probably due to differences in processing rather than to differences in dispersoid identity. These results also show that yttrium oxide, a nonradioactive oxide, is as suitable a dispersoid in a complex alloy base as thorium oxide.

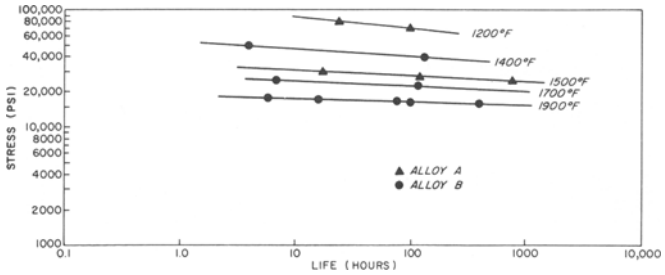

Fig. 6—Results of stress rupture tests performed on yttriated superalloys A and B.

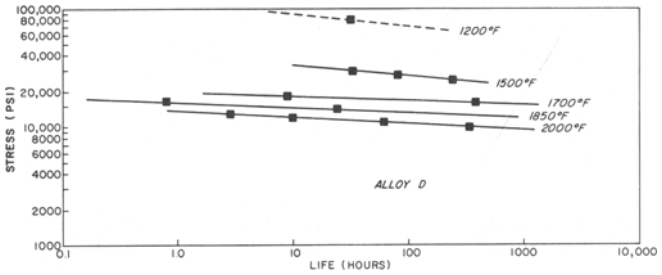

Fig. 7—Results of stress rupture tests performed on thoriated superalloy D.

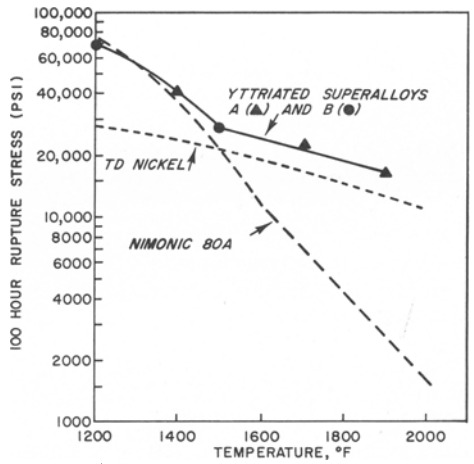

Fig. 8—Stress for 100 hr life in yttriated superalloys as a function of temperature.

An additional feature of the dispersion strengthened superalloy is seen in Fig. 10. Because the stress rupture curves of the dispersion strengthened superalloy are flatter than those of conventional superalloys at intermediate temperatures such as 1400°F, it follows that the dispersion strengthened superalloy is significantly stronger than either TD Nickel or NIMONIC 80A at longer times, such as 1000 hr. The effects of dispersion strengthening and precipitation hardening appear to augment each other at long times in this temperature range.

Tensile properties of yttriated alloys at room and elevated temperature are plotted as a function of temperature in Fig. 11 and listed in Table II. Also included in Fig. 11 are typical tensile strengths of TD Nickel and NIMONIC 80A.[26] Comparison of these curves again shows the temperature regions in which the γ' and oxide dispersion strengthening regimes predominate in the yttriated superalloys. The tensile strength of the yttri-

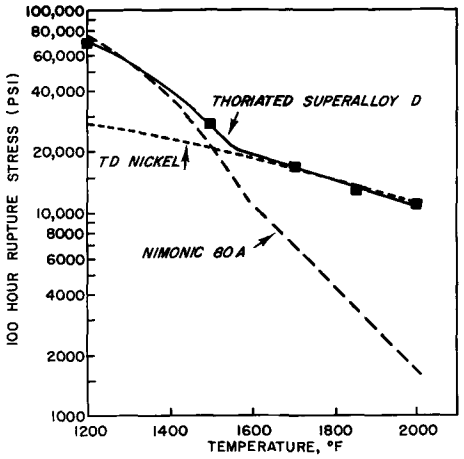

Fig. 9–Stress for 100 hr life in thoriated superalloy as a function of temperature.

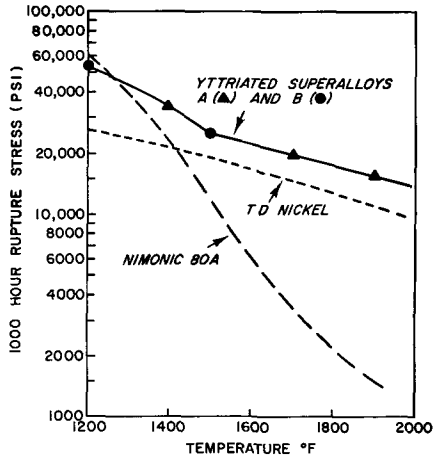

Fig. 10–Stress for 1000 hr life in yttriated superalloys as a function of temperature.

ated superalloy is somewhat lower than that of NIMONIC 80A at 1600°F. While this follows from the flatter slope of the stress rupture plot of the yttriated superalloy at this temperature, the lower level of the strength may be attributed to the fact that the soluble aluminum content in the yttriated superalloy, 0.92 wt pct, is lower than the 1.3 pct present in NIMONIC 80A.

Notched-unnotched combination stress rupture tests were performed on dispersion strengthened superalloy A at 1400° and 1900°F. Notch strengthening occurred at 1400°F as is common in the γ' strengthening region of nickel-base superalloys. There was no apparent effect of the notches at 1900°F; failures occurred in either the smooth or notched portions of the combination test bars depending on which section had the smaller cross section.

The dynamic elastic modulus, E, of the yttriated superalloy is plotted as a function of temperature in Fig. 12. Also given are values for NIMONIC 80A[26] and TD Nickel.[26] The modulus of the yttriated superalloy is slightly higher than values given for NIMONIC 80A and shows an identical variation with temperature. It is interesting that the modulus of the yttriated superalloy is about 50 pct higher than that of TD Nickel, even at 2000°F where the mechanical behavior of the two alloys is otherwise very similar. This test was performed

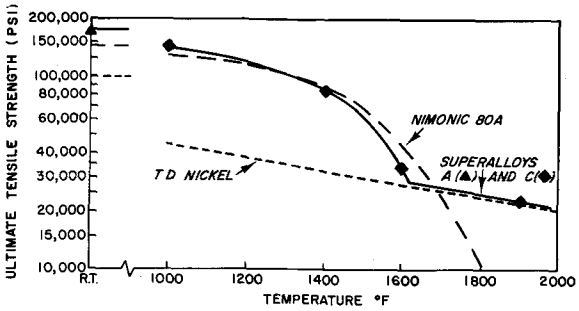

Fig. 11–Ultimate tensile strength of yttriated superalloys as a function of temperature.

Table II. Tensile Properties of Yttriated Nickel-Base Superalloys

Alloy	Test Temp.	0.2 Pct Offset Yield Stress, psi	Ultimate Tensile Strength, psi	Elongation, Pct	Red. of Area, Pct
C	Room Temp	129,000	175,000	9.0	13.5
A	1000°F	106,800	141,000	10.0	10.5
A	1400°F	81,200	84,400	25.0	32.5
A	1600°F	31,400	33,200	25.0	42.0
A	1900°F	20,900	22,800	9.0	19.0

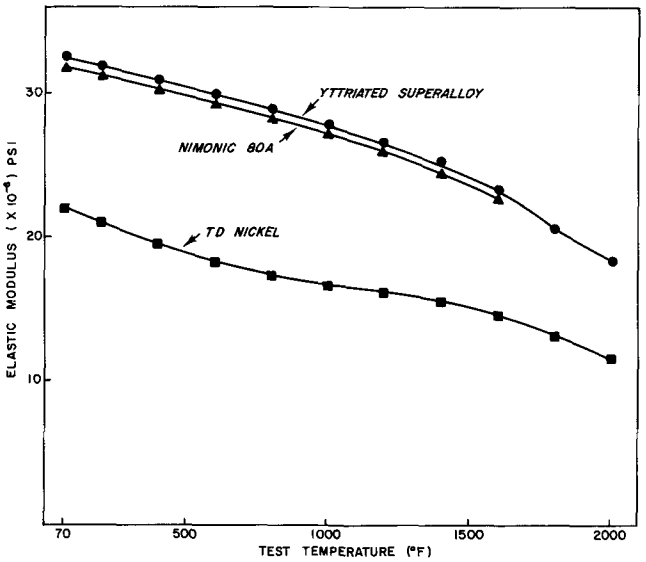

Fig. 12–Dynamic elastic modulus of yttriated superalloy as a function of temperature.

using a precision ground rod of 0.5 in. diam and 6 in. length. The density of the yttriated superalloy calculated from these dimensions and the weight of the rod is 8.09 g per cc.

Hot corrosion resistance of the dispersion strengthened superalloy was evaluated by sulfidation crucible tests and by cyclic oxidation tests. Results of these tests[27] are given in Table III along with data for Udimet*

*Registered Trademark of Special Metals, Inc.

500 and NIMONIC 80A. The sulfidation tests involved immersion at 1700°F in 90 pct Na_2SO_4-10 pct NaCl for 100 and 300 hr. Oxidation tests involved rapidly cycling from 2000°F to room temperature and back to 2000°F once a day with a total exposure time of 400 hr.

Table III. Hot Corrosion Results

Alloy	1700°F Sulfidation Tests (Crucible tests in 90 pct Na_2SO_4-10 pct NaCl) 100 hr Metal Loss, mils	100 hr Sulfide Subscale, mils	300 hr Metal Loss, mils	300 hr Sulfide Subscale, mils	2000°F Cyclic Oxidation 400 hr Descaled Weight Loss, mg/cm^2
Nimonic 80A	3	5	5	18	82
Udimet 500	–	–	23	14	69.3
Yttriated superalloy	3	0.7	3	1	44.3

The sulfidation resistance of the dispersion strengthened superalloy is superior to both NIMONIC 80A and Udimet 500. This is especially apparent in the 300 hr tests where the yttriated superalloy shows a sulfide subscale penetration of only 1 mil as opposed to 14 mil for Udimet 500 and 18 mil for NIMONIC 80A. In cyclic oxidation at 2000°F the descaled weight loss after 400 hr exposure shows the yttriated superalloy to be superior to Udimet 500 and NIMONIC 80A. It should be noted that the scale on the yttriated superalloy was adherent throughout the test while the scales on the other two alloys spalled continuously after 24 to 48 hr of exposure. This indicates that the superiority of the yttriated superalloy would be even greater with increasing exposure time in cyclic oxidation.

CONCLUSIONS

1) Mechanical alloying by dry high energy ball milling without a surface active addition has been used to produce homogeneous composite powder particles which are relatively coarse and free from detrimental contamination. The process involves recurrent cold welding of constituents to the ball surfaces and flaking off of the composite aggregates until all of the constituents are finely divided and uniformly distributed through the interior of each powder particle.

2) Mechanical alloying processing times of 40 hr or less are adequate to obtain suitably homogeneous powders.

3) Mechanical alloying can be used to combine fine particle dispersion strengthening with age hardening in a nickel-base superalloy. After canning, extrusion, and heat treatment, the product possesses the strength and stability of thoriated nickel at 1900°F and the very high rupture strength of a γ' hardened superalloy at 1400°F. At the same time the product has sulfidation and cyclic oxidation resistance as good as or superior to conventional superalloys of similar composition.

4) It has been found that yttria is as effective as thoria in dispersion strengthening complex nickel-base alloys. Use of yttria avoids any radioactivity problems associated with handling thoria.

5) In the temperature range 1300° to 1500°F the dispersion and precipitation hardening mechanisms augment each other in the nickel-base alloy. At lower temperatures and higher strain rates (lower rupture lives) precipitation hardening by γ' dominates, and at the higher temperatures and/or lower strain rates (higher rupture lives) dispersion strengthening is dominant.

REFERENCES

1. W. D. Coolidge: *Proc. Am. Inst. Elec. Eng.*, 1910, p. 961.
2. R. Irmann: *Metallurgia*, 1952, vol. 49, p. 125.
3. E. Gregory and N. J. Grant: *AIME Trans.*, 1954, vol. 200, p. 247.
4. F. V. Lenel, A. B. Backensto, Jr., and M. V. Rose: *AIME Trans.*, 1957, vol. 209, p. 124.
5. C. J. Leadbeater and discussion by E. Gregory: Symposium on Powder Metallurgy, 1954, Iron Steel Inst. Spec. Rept. No. 58, pp. 149-59, 357.
6. G. B. Alexander *et al.*: U.S. Patent No. 2,972,529, Feb. 21, 1961.
7. F. J. Anders, Jr.: U.S. Patent No. 3,159,908, Dec. 8, 1964.
8. E. Gregory and C. G. Goetzel: *Trans. TMS-AIME*, 1958, vol. 212, p. 868.
9. K. M. Zwilsky and N. J. Grant: *Trans. TMS-AIME*, 1961, vol. 221, p. 371.
10. V. A. Tracey and D. K. Worn: *Powder Met.*, 1962, no. 10, p. 34.
11. R. Murphy and N. J. Grant: *Powder Met.*, 1962, no. 10, p. 1.
12. C. J. Smithells: U.S. Patent No. 2,406,172, Aug. 20, 1946.
13. Dutch Patent No. 64030, Sept. 15, 1949.
14. J. C. Chaston: *J. Inst. Metals*, 1945, vol. 71, pp. 23-35.
15. L. J. Bonis and N. J. Grant: *Trans. TMS-AIME*, 1962, vol. 224, p. 308.
16. H. Spengler: *Metall.*, 1964, vol. 18, p. 727.
17. M. Adachi and N. J. Grant: *Trans. TMS-AIME*, 1960, vol. 218, p. 881.
18. G. H. Howe: *Powder Metallurgy*, J. Wulff, ed., p. 530, ASM, 1942.
19. A. Steiner and K. L. Komarek: *Trans. TMS-AIME*, 1964, vol. 230, p. 786.
20. H. Wadham: *J. Oil Colour Chemists Assoc.*, 1964, p. 728.
21. A. Szegvari: U.S. Patent No. 2,764,359, Sept. 25, 1956.
22. A. M. Gaudin: *Principles of Mineral Dressing*, p. 106, McGraw Hill Book Co., New York, 1939.
23. F. C. Kelly: *Weld. J. N. Y.*, 1951, vol. 30, p. 728.
24. S. L. Hoyt: *AIME Trans.*, 1930, vol. 89, p. 9, see esp. p. 25.
25. G. S. Ansell and J. Weertman: *Trans. TMS-AIME*, 1959, vol. 215, p. 838.
26. High Temperature, High Strength Nickel-Base Alloys, The International Nickel Co., Inc., New York, 1964. Note: The values for the properties of TD Nickel are given only for reference and represent an average of the numbers reported in the open literature and in manufacturers' pamphlets for varying bar sizes of this alloy.
27. J. W. Schultz: The International Nickel Co., Inc., Paul D. Merica Research Laboratory, Sterling Forest, Suffern, N.Y., private communication, 1969.